

A novel model for biofilm growth and its resolution by using the hybrid immersed interface-level set method

Patricio Cumsille Atala

Juan A. Asenjo & Carlos Conca

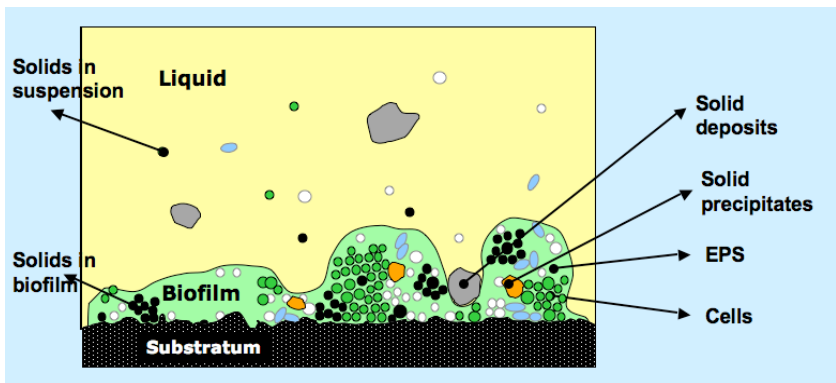
Applied Mathematics Group - Basic Sciences Department - University of Bío-Bío
Chillán-Chile

&

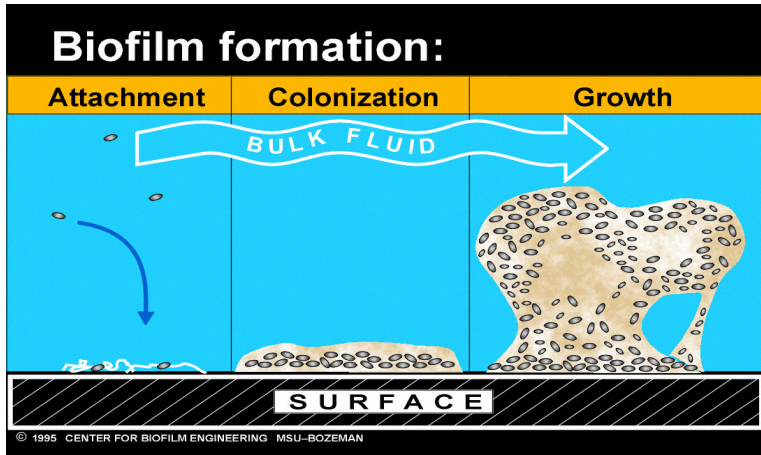
Centre for Biotechnology and Bioengineering - University of Chile

Congress Conca 60 - Workshop Chile-Euskadi
Basque Center for Applied Mathematics (BCAM) - Bilbao

What is a biofilm?



Biofilm formation



Why to study a biofilm?

Applications

- Bioremediation: technologies to assist the remediation of field sites contaminated with fuel hydrocarbons.
- Waste water treatment
- **Bioleaching**: A method to extract metals (such as copper) from the ore using only natural ingredients which are very easy to find in the environment: water, air and bacteria.

Why to study a biofilm?

Applications

- Bioremediation: technologies to assist the remediation of field sites contaminated with fuel hydrocarbons.
- Waste water treatment
- **Bioleaching**: A method to extract metals (such as copper) from the ore using only natural ingredients which are very easy to find in the environment: water, air and bacteria.

Why to study a biofilm?

Applications

- Bioremediation: technologies to assist the remediation of field sites contaminated with fuel hydrocarbons.
- Waste water treatment
- **Bioleaching**: A method to extract metals (such as copper) from the ore using only natural ingredients which are very easy to find in the environment: water, air and bacteria.

Biofilm modeling

Generalities

Basic biofilm models are based upon three principles:

- 1 Transport mechanisms (advection, diffusion): for bringing nutrients into the biofilm.
- 2 Consumption and growing mechanisms.
- 3 Mechanisms for biofilm necrosis and loss.

New: Modeling of the *biofilm front* based on the Hele-Shaw flow (fingering instabilities).

Biofilm modeling

Generalities

Basic biofilm models are based upon three principles:

- 1 Transport mechanisms (advection, diffusion): for bringing nutrients into the biofilm.
- 2 Consumption and growing mechanisms.
- 3 Mechanisms for biofilm necrosis and loss.

New: Modeling of the *biofilm front* based on the Hele-Shaw flow (fingering instabilities).

Biofilm modeling

Generalities

Basic biofilm models are based upon three principles:

- 1 Transport mechanisms (advection, diffusion): for bringing nutrients into the biofilm.
- 2 Consumption and growing mechanisms.
- 3 Mechanisms for biofilm necrosis and loss.

New: Modeling of the *biofilm front* based on the Hele-Shaw flow (fingering instabilities).

Biofilm modeling

Generalities

Basic biofilm models are based upon three principles:

- 1 Transport mechanisms (advection, diffusion): for bringing nutrients into the biofilm.
- 2 Consumption and growing mechanisms.
- 3 Mechanisms for biofilm necrosis and loss.

New: Modeling of the *biofilm front* based on the Hele-Shaw flow (fingering instabilities).

Biofilm modeling

Generalities

Basic biofilm models are based upon three principles:

- 1 Transport mechanisms (advection, diffusion): for bringing nutrients into the biofilm.
- 2 Consumption and growing mechanisms.
- 3 Mechanisms for biofilm necrosis and loss.

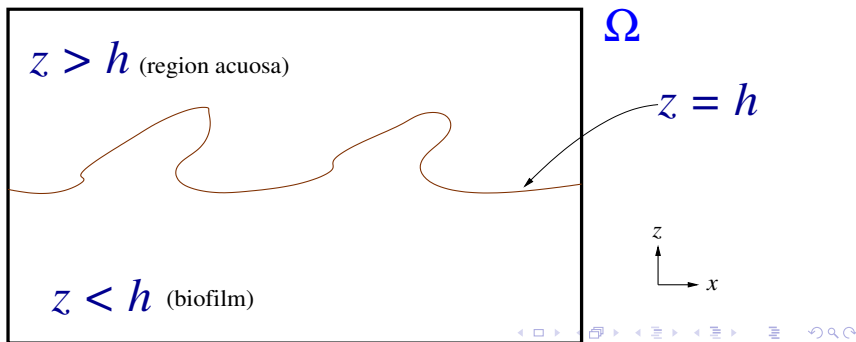
New: Modeling of the *biofilm front* based on the Hele-Shaw flow (fingering instabilities).

Modeling

Let $\Omega \subset \mathbb{R}^2$ be the rectangle $\Omega = (0, L_x) \times (0, L_z)$, divided into two subregions: the biofilm compartment $z < h(x, t)$ and the liquid compartment $z > h(x, t)$, with curve interface $z = h(x, t)$ (the interface need not to be expressible as a function of x).

Modeling

Let $\Omega \subset \mathbb{R}^2$ be the rectangle $\Omega = (0, L_x) \times (0, L_z)$, divided into two subregions: the biofilm compartment $z < h(x, t)$ and the liquid compartment $z > h(x, t)$, with curve interface $z = h(x, t)$ (the interface need not to be expressible as a function of x).



Hele-Shaw flow model

The biofilm is modeled as a homogeneous viscous fluid, which satisfies Darcy law

$$\mathbf{u} = -\nabla p$$

\mathbf{u} , p velocity and pressure resp. The biofilm may be growing or decaying, so that

$$\nabla \cdot \mathbf{u} = g \quad \text{in } \Omega_2(t)$$

for some g prescribed *growing function*. Note that g depends on the *substrate uptake rate* $U(S)$, i.e. $g = g(U)$, where S is a single limiting substrate (e.g., oxygen or glucose).

Hele-Shaw flow model

The biofilm is modeled as a homogeneous viscous fluid, which satisfies Darcy law

$$\mathbf{u} = -\nabla p$$

\mathbf{u} , p velocity and pressure resp. The biofilm may be growing or decaying, so that

$$\nabla \cdot \mathbf{u} = g \quad \text{in } \Omega_2(t)$$

for some g prescribed *growing function*. Note that g depends on the *substrate uptake rate* $U(S)$, i.e. $g = g(U)$, where S is a single limiting substrate (e.g., oxygen or glucose).

Hele-Shaw flow model

The biofilm is modeled as a homogeneous viscous fluid, which satisfies Darcy law

$$\mathbf{u} = -\nabla p$$

\mathbf{u} , p velocity and pressure resp. The biofilm may be growing or decaying, so that

$$\nabla \cdot \mathbf{u} = g \quad \text{in } \Omega_2(t)$$

for some g prescribed *growing function*. Note that g depends on the *substrate uptake rate* $U(S)$, i.e. $g = g(U)$, where S is a single limiting substrate (e.g., oxygen or glucose).

The Hele-Shaw flow (revisited)

Pressure equations

$$-\nabla^2 p = \begin{cases} g(U) & \text{in the biofilm region,} \\ 0 & \text{in the liquid region.} \end{cases}$$

The transmissions conditions on the interface $\Gamma(t)$ are:

$$\begin{cases} [p] = d_0 \kappa & \text{(Laplace-Young condition)} \\ \left[\frac{\partial p}{\partial n} \right] = 0 & \text{(kinematic condition)} \end{cases}$$

d_0 , κ are the *amalgamated surface tension coefficient* and the *mean curvature* resp.

The Hele-Shaw flow (revisited)

Pressure equations

$$-\nabla^2 p = \begin{cases} g(U) & \text{in the biofilm region,} \\ 0 & \text{in the liquid region.} \end{cases}$$

The transmissions conditions on the interface $\Gamma(t)$ are:

$$\begin{cases} [p] = d_0 \kappa & \text{(Laplace-Young condition)} \\ \left[\frac{\partial p}{\partial n} \right] = 0 & \text{(kinematic condition)} \end{cases}$$

d_0 , κ are the *amalgamated surface tension coefficient* and the *mean curvature* resp.

Substrate equations

$$S_t + \nabla \cdot (S\mathbf{u}) - \frac{D_S T}{L_Z^2} \nabla^2 S = 0 \quad \text{in } \Omega_1(t),$$

$$S_t + \nabla \cdot (S\mathbf{u}) - \frac{D_S T}{L_Z^2} \nabla^2 S = -U(S) \quad \text{in } \Omega_2(t).$$

The transmissions conditions on the interface $\Gamma(t)$ are the "natural conditions":

$$\begin{cases} [S] = 0 \\ \left[\frac{\partial S}{\partial n} \right] = 0 \end{cases}$$

Substrate equations

$$S_t + \nabla \cdot (S\mathbf{u}) - \frac{D_S T}{L_Z^2} \nabla^2 S = 0 \quad \text{in } \Omega_1(t),$$

$$S_t + \nabla \cdot (S\mathbf{u}) - \frac{D_S T}{L_Z^2} \nabla^2 S = -U(S) \quad \text{in } \Omega_2(t).$$

The transmissions conditions on the interface $\Gamma(t)$ are the "natural conditions":

$$\begin{cases} [S] = 0 \\ \left[\frac{\partial S}{\partial n} \right] = 0 \end{cases}$$

Modeling of the substrate uptake rate function

Monod function

A typical choice for U is the *Monod* function

$$U(S) = \underbrace{\left(\frac{TU_m}{S_m} \right)}_{\nu} \delta_U (1 + \mu) \frac{S}{S + K}$$

where T , U_m , S_m , μ , K are the *time scale of biofilm growth*, *reaction rate coefficient*, *maximum substrate concentration*, *maintenance coefficient* and *dimensionless half-saturation*, resp. This form is also often used for the growing function g :

$$g(U(S)) = \frac{\nu S_m}{U_m} \delta_g \mu_m \left[(1 + \mu) \frac{S}{S + K} - \mu \right]$$

Finally, δ_U and δ_g are scaling parameters.

Modeling of the substrate uptake rate function

Monod function

A typical choice for U is the *Monod* function

$$U(S) = \underbrace{\left(\frac{TU_m}{S_m} \right)}_{\nu} \delta_U (1 + \mu) \frac{S}{S + K}$$

where T , U_m , S_m , μ , K are the *time scale of biofilm growth*, *reaction rate coefficient*, *maximum substrate concentration*, *maintenance coefficient* and *dimensionless half-saturation*, resp. This form is also often used for the growing function g :

$$g(U(S)) = \frac{\nu S_m}{U_m} \delta_g \mu_m \left[(1 + \mu) \frac{S}{S + K} - \mu \right]$$

Finally, δ_U and δ_g are scaling parameters.

External boundary conditions

For the pressure:

$$\left\{ \begin{array}{l} p|_{z=H} = 0, \\ p \text{ periodic in } x \text{ direction.} \end{array} \right. \quad \frac{\partial p}{\partial z} \Big|_{z=0} = 0,$$

For the substrate:

$$\left\{ \begin{array}{l} S|_{z=H} = 1, \\ S \text{ periodic in } x \text{ direction.} \end{array} \right. \quad \frac{\partial S}{\partial z} \Big|_{z=0} = 0,$$

External boundary conditions

For the pressure:

$$\left\{ \begin{array}{l} p|_{z=H} = 0, \\ p \text{ periodic in } x \text{ direction.} \end{array} \right. \quad \frac{\partial p}{\partial z} \Big|_{z=0} = 0,$$

For the substrate:

$$\left\{ \begin{array}{l} S|_{z=H} = 1, \\ S \text{ periodic in } x \text{ direction.} \end{array} \right. \quad \frac{\partial S}{\partial z} \Big|_{z=0} = 0,$$

The full biofilm model

Main difficulties

Key issue

Evolution of the biofilm front is a *unknown* of the model \Rightarrow problem highly *non-linear*. We so deal with a *free boundary value problem*.

Generalized solutions

The presence of the interface implies that the solution is defined in a weak sense (it is discontinuous). Thus, well-posedness for this problem is a non-trivial issue.

Main novelty

Intensive numerical simulations were successfully carried out. This is achieved by coupling the level set method and the immersed interface method.

The full biofilm model

Main difficulties

Key issue

Evolution of the biofilm front is a *unknown* of the model \Rightarrow problem highly *non-linear*. We so deal with a *free boundary value problem*.

Generalized solutions

The presence of the interface implies that the solution is defined in a weak sense (it is discontinuous). Thus, well-posedness for this problem is a non-trivial issue.

Main novelty

Intensive numerical simulations were successfully carried out. This is achieved by coupling the level set method and the immersed interface method.

The full biofilm model

Main difficulties

Key issue

Evolution of the biofilm front is a *unknown* of the model \Rightarrow problem highly *non-linear*. We so deal with a *free boundary value problem*.

Generalized solutions

The presence of the interface implies that the solution is defined in a weak sense (it is discontinuous). Thus, well-posedness for this problem is a non-trivial issue.

Main novelty

Intensive numerical simulations were successfully carried out. This is achieved by coupling the level set method and the immersed interface method.

Numerical method for the interface evolution (1/3)

The level set method

Let $\phi(x, z, t)$ be satisfying $\phi(x, z, t) > 0$ for (x, z) in the liquid region and $\phi(x, z, t) < 0$ for (x, z) in the biofilm region. Then, by continuity $\phi(x, z, t)$ satisfies

$$(x, z) \in \text{Biofilm front} \Leftrightarrow \phi(x, z, t) = 0.$$

Thus, the motion of the biofilm front is modeled by the *level set equation*:

$$\begin{cases} \frac{\partial \phi}{\partial t} + \mathbf{u} \cdot \nabla \phi = 0, & \text{for } (x, z) \in \Omega, t > 0, \\ \phi(x, z, 0) = \phi_0(x, z), & \text{for } (x, z) \in \Omega, \end{cases}$$

where $\phi_0(x, z)$ implicitly defines the initial biofilm front.

Numerical method for the interface evolution (1/3)

The level set method

Let $\phi(x, z, t)$ be satisfying $\phi(x, z, t) > 0$ for (x, z) in the liquid region and $\phi(x, z, t) < 0$ for (x, z) in the biofilm region. Then, by continuity $\phi(x, z, t)$ satisfies

$$(x, z) \in \text{Biofilm front} \Leftrightarrow \phi(x, z, t) = 0.$$

Thus, the motion of the biofilm front is modeled by the *level set equation*:

$$\begin{cases} \frac{\partial \phi}{\partial t} + \mathbf{u} \cdot \nabla \phi = 0, & \text{for } (x, z) \in \Omega, t > 0, \\ \phi(x, z, 0) = \phi_0(x, z), & \text{for } (x, z) \in \Omega, \end{cases}$$

where $\phi_0(x, z)$ implicitly defines the initial biofilm front.

Numerical method for the interface evolution (1/3)

The level set method

Let $\phi(x, z, t)$ be satisfying $\phi(x, z, t) > 0$ for (x, z) in the liquid region and $\phi(x, z, t) < 0$ for (x, z) in the biofilm region. Then, by continuity $\phi(x, z, t)$ satisfies

$$(x, z) \in \text{Biofilm front} \Leftrightarrow \phi(x, z, t) = 0.$$

Thus, the motion of the biofilm front is modeled by the *level set equation*:

$$\begin{cases} \frac{\partial \phi}{\partial t} + \mathbf{u} \cdot \nabla \phi = 0, & \text{for } (x, z) \in \Omega, t > 0, \\ \phi(x, z, 0) = \phi_0(x, z), & \text{for } (x, z) \in \Omega, \end{cases}$$

where $\phi_0(x, z)$ implicitly defines the initial biofilm front.

Numerical method for the interface evolution (2/3)

The reinitialization process

In the level set method $\phi(x, z, t)$ corresponds to the signed normal distance from the point (x, z) to the interface $\Gamma(t)$. Although the level set equation transports the interface at the right velocity \mathbf{u} , it does not preserve ϕ as a distance function. To overcome this difficulty, we have used the reinitialization process:

$$\begin{cases} \psi_\tau + \text{Sg}(\phi)(|\nabla\psi| - 1) = 0, \\ \psi(x, z, 0) = \phi(x, z, t), \end{cases}$$

where $\psi(x, z, t)$ corresponds to the level set function at time t_{n+1} , and $\text{Sg}(\phi)$ is the one dimensional sign function composed with ϕ .

Numerical method for the interface evolution (2/3)

The reinitialization process

In the level set method $\phi(x, z, t)$ corresponds to the signed normal distance from the point (x, z) to the interface $\Gamma(t)$. Although the level set equation transports the interface at the right velocity \mathbf{u} , it does not preserve ϕ as a distance function. To overcome this difficulty, we have used the reinitialization process:

$$\begin{cases} \psi_\tau + \text{Sg}(\phi)(|\nabla\psi| - 1) = 0, \\ \psi(x, z, 0) = \phi(x, z, t), \end{cases}$$

where $\phi(x, z, t)$ corresponds to the level set function at time t_{n+1} , and $\text{Sg}(\phi)$ is the one dimensional sign function composed with ϕ .

Numerical method for the interface evolution (3/3)

Numerical methods for the level set equations

We apply this process every 15 time iterations, taking care of obtaining a steady state solution in order to numerically obtain that $|\nabla\psi| \approx 1$. The new function ψ has the same level sets as ϕ and is the signed normal distance to the interface.

Both Hamilton-Jacobi equations are solved by coupling a second-order TVD Runge-Kutta method to update ϕ (resp. ψ) from time t_n to t_{n+1} (resp. τ_n to τ_{n+1}), with a second-order ENO approximation to $\nabla\phi$ (resp. $\nabla\psi$). For an overview of the level set method see [Osher and Fedkiw, 2003].

Numerical method for the interface evolution (3/3)

Numerical methods for the level set equations

We apply this process every 15 time iterations, taking care of obtaining a steady state solution in order to numerically obtain that $|\nabla\psi| \approx 1$. The new function ψ has the same level sets as ϕ and is the signed normal distance to the interface.

Both Hamilton-Jacobi equations are solved by coupling a second-order TVD Runge-Kutta method to update ϕ (resp. ψ) from time t_n to t_{n+1} (resp. τ_n to τ_{n+1}), with a second-order ENO approximation to $\nabla\phi$ (resp. $\nabla\psi$). For an overview of the level set method see [Osher and Fedkiw, 2003].

Numerical method for the pressure equations

Immersed Interface Method (IIM)

- The IIM [LeVeque and Li, 1994] deals with general interface conditions. This method is comparable, but more general than the immersed boundary method [Peskin, 1977].
- The discontinuities of the solution and/or coefficients are imposed in the standard method, by modifying it at *irregular grid points*, i.e., at grid points whose standard five-point stencil centered around it, is located in both sides of the interface (see figure in the next slide).
- If coefficients of the equation are continuous (which is our case), the IIM just adds a correction term in the right-hand side of the discretized equation at the irregular grid points.

Numerical method for the pressure equations

Immersed Interface Method (IIM)

- The IIM [LeVeque and Li, 1994] deals with general interface conditions. This method is comparable, but more general than the immersed boundary method [Peskin, 1977].
- The discontinuities of the solution and/or coefficients are imposed in the standard method, by modifying it at *irregular grid points*, i.e., at grid points whose standard five-point stencil centered around it, is located in both sides of the interface (see figure in the next slide).
- If coefficients of the equation are continuous (which is our case), the IIM just adds a correction term in the right-hand side of the discretized equation at the irregular grid points.

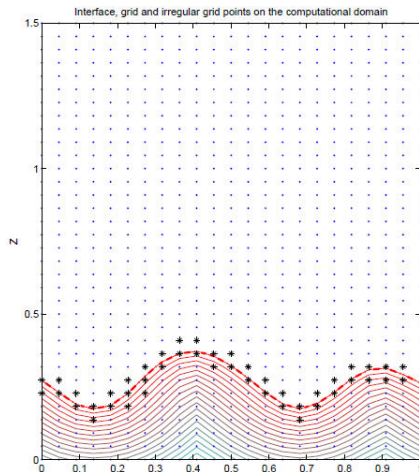
Numerical method for the pressure equations

Immersed Interface Method (IIM)

- The IIM [LeVeque and Li, 1994] deals with general interface conditions. This method is comparable, but more general than the immersed boundary method [Peskin, 1977].
- The discontinuities of the solution and/or coefficients are imposed in the standard method, by modifying it at *irregular grid points*, i.e., at grid points whose standard five-point stencil centered around it, is located in both sides of the interface (see figure in the next slide).
- If coefficients of the equation are continuous (which is our case), the IIM just adds a correction term in the right-hand side of the discretized equation at the irregular grid points.

Immersed Interface Method

Interface (dashed line), regular grid (points) and irregular grid points (stars)



Algorithm

- Step 1.** $n \leftarrow 0$. Initialize the initial biofilm front, i.e., set $\phi(x, z, t = 0)$. At $t = 0$ the substrate is at its maximum level and uniformly distributed in the space, i.e. $S(x, z, t = 0) = 1$.
- Step 2. Solve the pressure equations, and compute $\mathbf{u} = -\nabla p$ based on the IIM at time $t_n = n\Delta t$.
- Step 3. Solve the substrate equations at time t_n .
- Step 4. Update the position of the interface with the velocity field $\mathbf{u} = -\nabla p$, by solving the level-set equation. Reinitialize the level-set function every 15 time steps.
- Step 5. Update $n \leftarrow n + 1$ and repeat Step 2 to Step 5 to let evolve the system.

Algorithm

- Step 1.** $n \leftarrow 0$. Initialize the initial biofilm front, i.e., set $\phi(x, z, t = 0)$. At $t = 0$ the substrate is at its maximum level and uniformly distributed in the space, i.e. $S(x, z, t = 0) = 1$.
- Step 2.** Solve the pressure equations, and compute $\mathbf{u} = -\nabla p$ based on the IIM at time $t_n = n\Delta t$.
- Step 3. Solve the substrate equations at time t_n .
- Step 4. Update the position of the interface with the velocity field $\mathbf{u} = -\nabla p$, by solving the level-set equation. Reinitialize the level-set function every 15 time steps.
- Step 5. Update $n \leftarrow n + 1$ and repeat Step 2 to Step 5 to let evolve the system.

Algorithm

- Step 1.** $n \leftarrow 0$. Initialize the initial biofilm front, i.e., set $\phi(x, z, t = 0)$. At $t = 0$ the substrate is at its maximum level and uniformly distributed in the space, i.e. $S(x, z, t = 0) = 1$.
- Step 2.** Solve the pressure equations, and compute $\mathbf{u} = -\nabla p$ based on the IIM at time $t_n = n\Delta t$.
- Step 3.** Solve the substrate equations at time t_n .
- Step 4.** Update the position of the interface with the velocity field $\mathbf{u} = -\nabla p$, by solving the level-set equation. Reinitialize the level-set function every 15 time steps.
- Step 5.** Update $n \leftarrow n + 1$ and repeat Step 2 to Step 5 to let evolve the system.

Algorithm

- Step 1.** $n \leftarrow 0$. Initialize the initial biofilm front, i.e., set $\phi(x, z, t = 0)$. At $t = 0$ the substrate is at its maximum level and uniformly distributed in the space, i.e. $S(x, z, t = 0) = 1$.
- Step 2.** Solve the pressure equations, and compute $\mathbf{u} = -\nabla p$ based on the IIM at time $t_n = n\Delta t$.
- Step 3.** Solve the substrate equations at time t_n .
- Step 4.** Update the position of the interface with the velocity field $\mathbf{u} = -\nabla p$, by solving the level-set equation. Reinitialize the level-set function every 15 time steps.
- Step 5.** Update $n \leftarrow n + 1$ and repeat Step 2 to Step 5 to let evolve the system.

Algorithm

- Step 1.** $n \leftarrow 0$. Initialize the initial biofilm front, i.e., set $\phi(x, z, t = 0)$. At $t = 0$ the substrate is at its maximum level and uniformly distributed in the space, i.e. $S(x, z, t = 0) = 1$.
- Step 2.** Solve the pressure equations, and compute $\mathbf{u} = -\nabla p$ based on the IIM at time $t_n = n\Delta t$.
- Step 3.** Solve the substrate equations at time t_n .
- Step 4.** Update the position of the interface with the velocity field $\mathbf{u} = -\nabla p$, by solving the level-set equation. Reinitialize the level-set function every 15 time steps.
- Step 5.** Update $n \leftarrow n + 1$ and repeat Step 2 to Step 5 to let evolve the system.

Parameters

We have taken the following common parameters in our simulations [Picioreanu et al., 2000]:

Parameter	Symbol	Value	Units
Time scale of biofilm growth	T	1000	s
Monod half-saturation constant	K_S	$3.5 \cdot 10^{-4}$	kg m^{-3}
Diffusion coefficient	D_S	$2.3 \cdot 10^{-9}$	$\text{m}^2 \text{s}^{-1}$
Surface tension coefficient in water	γ	$72.8 \cdot 10^{-3}$	kg s^{-2}
Maximum specific growth rate	μ_m	$1.5 \cdot 10^{-5}$	s^{-1}

A key parameter is the ratio (maximum biomass growth rate)/(maximum internal transport rate of substrate) [Picioreanu et al., 1998b], which determines the biofilm heterogeneity. The growth ratio, G , is computed as $G = L_Z^2 U_m / (D_S S_m)$. By setting $S_m = 4$ and 100 mg/L , G is taken as 395 and 16. Moreover, U_m and d_0 are computed accordingly to these values.

Parameters

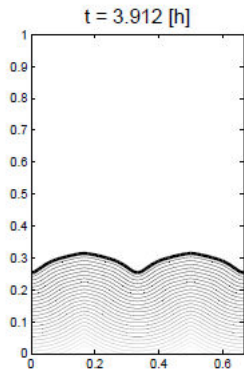
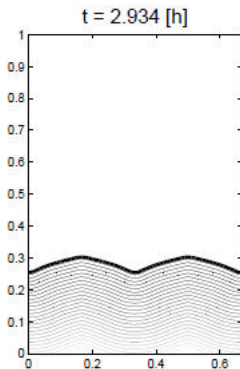
We have taken the following common parameters in our simulations [Picioreanu et al., 2000]:

Parameter	Symbol	Value	Units
Time scale of biofilm growth	T	1000	s
Monod half-saturation constant	K_S	$3.5 \cdot 10^{-4}$	kg m^{-3}
Diffusion coefficient	D_S	$2.3 \cdot 10^{-9}$	$\text{m}^2 \text{s}^{-1}$
Surface tension coefficient in water	γ	$72.8 \cdot 10^{-3}$	kg s^{-2}
Maximum specific growth rate	μ_m	$1.5 \cdot 10^{-5}$	s^{-1}

A key parameter is the ratio (maximum biomass growth rate)/(maximum internal transport rate of substrate) [Picioreanu et al., 1998b], which determines the biofilm heterogeneity. The growth ratio, G , is computed as $G = L_Z^2 U_m / (D_S S_m)$. By setting $S_m = 4$ and 100 mg/L , G is taken as 395 and 16. Moreover, U_m and d_0 are computed accordingly to these values.

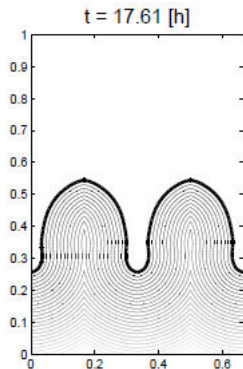
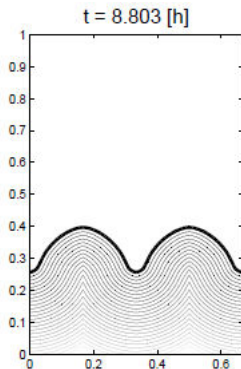
Numerical simulation for a transport-limited regime

Fingering formation



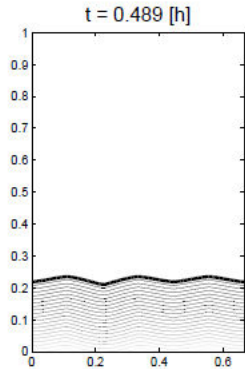
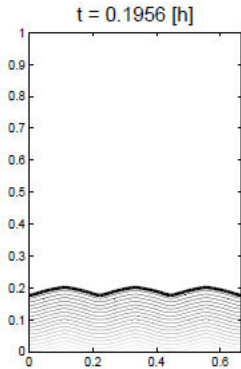
Numerical simulation for a transport-limited regime

Fingering formation



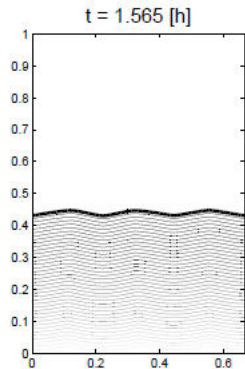
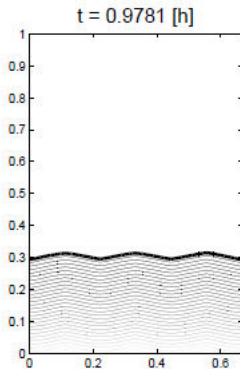
Numerical simulation for a growth-limited regime

Compact-shaped biofilm



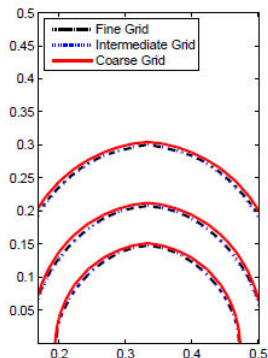
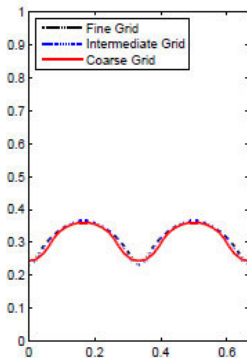
Numerical simulation for a growth-limited regime

Compact-shaped biofilm



Grid refinement analysis

For two simulations



Conclusions

- Development of a new model that predict real biofilm behavior (finger-like, as well as, more compact structures, depending on the environmental conditions).
- Development of sophisticated numerical techniques (the IIM coupled to the level-set method) in order to evaluate the model.
- We could consider the flow field induced by the liquid and not only by the biofilm growth.
- We could consider two or more substrates as well as biofilm systems with multiple species.
- We could consider biofilm detachment, which also determines biofilm structure.
- In addition, we could consider that the fluid dynamics is governed by e.g. Navier-Stokes equations.

Conclusions

- Development of a new model that predict real biofilm behavior (finger-like, as well as, more compact structures, depending on the environmental conditions).
- Development of sophisticated numerical techniques (the IIM coupled to the level-set method) in order to evaluate the model.
- We could consider the flow field induced by the liquid and not only by the biofilm growth.
- We could consider two or more substrates as well as biofilm systems with multiple species.
- We could consider biofilm detachment, which also determines biofilm structure.
- In addition, we could consider that the fluid dynamics is governed by e.g. Navier-Stokes equations.

Conclusions

- Development of a new model that predict real biofilm behavior (finger-like, as well as, more compact structures, depending on the environmental conditions).
- Development of sophisticated numerical techniques (the IIM coupled to the level-set method) in order to evaluate the model.
- We could consider the flow field induced by the liquid and not only by the biofilm growth.
- We could consider two or more substrates as well as biofilm systems with multiple species.
- We could consider biofilm detachment, which also determines biofilm structure.
- In addition, we could consider that the fluid dynamics is governed by e.g. Navier-Stokes equations.

Conclusions

- Development of a new model that predict real biofilm behavior (finger-like, as well as, more compact structures, depending on the environmental conditions).
- Development of sophisticated numerical techniques (the IIM coupled to the level-set method) in order to evaluate the model.
- We could consider the flow field induced by the liquid and not only by the biofilm growth.
- We could consider two or more substrates as well as biofilm systems with multiple species.
- We could consider biofilm detachment, which also determines biofilm structure.
- In addition, we could consider that the fluid dynamics is governed by e.g. Navier-Stokes equations.

Conclusions

- Development of a new model that predict real biofilm behavior (finger-like, as well as, more compact structures, depending on the environmental conditions).
- Development of sophisticated numerical techniques (the IIM coupled to the level-set method) in order to evaluate the model.
- We could consider the flow field induced by the liquid and not only by the biofilm growth.
- We could consider two or more substrates as well as biofilm systems with multiple species.
- We could consider biofilm detachment, which also determines biofilm structure.
- In addition, we could consider that the fluid dynamics is governed by e.g. Navier-Stokes equations.

Conclusions

- Development of a new model that predict real biofilm behavior (finger-like, as well as, more compact structures, depending on the environmental conditions).
- Development of sophisticated numerical techniques (the IIM coupled to the level-set method) in order to evaluate the model.
- We could consider the flow field induced by the liquid and not only by the biofilm growth.
- We could consider two or more substrates as well as biofilm systems with multiple species.
- We could consider biofilm detachment, which also determines biofilm structure.
- In addition, we could consider that the fluid dynamics is governed by e.g. Navier-Stokes equations.

Some references



P. Cumsille, J. A. Asenjo, and C. Conca (2014).

A novel model for biofilm growth and its resolution by using the hybrid immersed interface-level set method.

Comput. Math. Appl., 67 (2014), pp. 34–51.



LeVeque, R. J. and Li, Z. L. (1994).

The immersed interface method for elliptic equations with discontinuous coefficients and singular sources.

SIAM J. Numer. Anal., 31(4):1019–1044.





S. Osher, R. Fedkiw (2003)

Level set methods and dynamic implicit surfaces

Vol. 153 of Applied Mathematical Sciences, Springer-Verlag, New York, 2003.

Some references

-  Peskin, C. S. (1977).
Numerical analysis of blood flow in the heart.
J. Computational Phys., 25(3):220–252.
-  Picioreanu, C., van Loosdrecht, M. C. M., and Heijnen, J. J. (1998a).
Mathematical modeling of biofilm structure with a hybrid differential-discrete cellular automaton approach.
Biotechnol. Bioeng., 58(1):101–116.

Some references



Picioreanu, C., van Loosdrecht, M. C. M., and Heijnen, J. J. (1998b).

A new combined differential-discrete cellular automaton approach for biofilm modeling: Application for growth in gel beads.

Biotechnol. Bioeng., 57(6):718–731.



Picioreanu, C., van Loosdrecht, M. C. M., and Heijnen, J. J. (2000).

Effect of diffusive and convective substrate transport on biofilm structure formation: a two-dimensional modeling study.

Biotechnol. Bioeng., 69(5):504–515.

Acknowledgments

This work was partially supported by Millennium Scientific Initiative under grant number ICM P05-001-F. The work of first author was also partially supported by Chilean Government Fondecyt-Conicyt Program under grant number 11080222 and by Universidad del Bío-Bío (grant DIUBB 121909 GI/C).

Thank you for your attention!!